

the case with fish exudate. Similarly, reduced size at maturity in the TMA treatment was not associated with earlier maturation, as it was for fish exudate. TMA caused a decrease in fitness-related traits, as might any unspecific, mildly toxic chemical substance. In contrast, fish exudate brought about the expected shifts toward earlier reproduction and more but smaller offspring. Although the experiments differed in several respects (clones used, food level), the direction of responses was consistent in both.

The concentrations used in this study were based on the results of Boriss et al. (1999), so that the lower level was chosen to represent TMA concentration in naturally produced fish exudate and the higher to match that which was reported to induce pronounced migration behavior. The lower concentrations used (10–20  $\mu\text{M}$ ) produced rather weak effects, but these effects were in the same direction as the effects of higher TMA concentrations. It is unlikely that even lower concentrations would produce effects similar to the effects of fish exudate. A study by Reede (1995) showed that the response of life history traits to fish kairomone increased with concentration, and the reversal of that trend was never observed.

I conclude that TMA is not the substance triggering antipredatory life history shifts in *Daphnia*.

<sup>1</sup> Corresponding author (Olga.Sakwinska@unibas.ch).

#### Acknowledgments

I thank Luc De Meester, Dieter Ebert, Tom Little, Ian Sanders, Steve Stearns, Alan Tessier, and an anonymous reviewer for helpful comments on the manuscript. Kerstin Bittner kindly helped with getting the clones.

The work was supported by Swiss Nationalfond grant 31-43324-95.

## Some considerations of the <sup>210</sup>Pb constant rate of supply (CRS) dating model

**Abstract**—One of the most widely used radionuclides in the study of recent sedimentation processes is <sup>210</sup>Pb. Its depth profile in sediments is used as input for various dating models, which provide chronologies, mass fluxes, and sedimentation rates. In this work we revisited the CRS (constant rate of supply) model, widely used for dating sediments through <sup>210</sup>Pb. A more general hypothesis (periodic flux [PF]) was proposed and, although it confirmed the validity of CRS chronology, a detailed analysis of the mass sedimentation formula pointed out an inconsistency of the cited model. A new mass sedimentation formula was proposed and validated with a lake sediment core and four marine sediment cores.

Lead-210 is one of the most widely used radionuclides in recent radio-geochronology studies. This is basically due to its appropriate half-life ( $T_{1/2} = 22.3$  yr), which is suitable for studying sedimentary processes that have taken place during the last 100–150 yr and to the assumption that its atmospheric flux is constant, which permits relatively simple

Zoology Institute  
University of Basel  
Rheinsprung 9  
CH-4051 Basle, Switzerland

#### References

- BORISS, H., M. BOERSMA, AND K. H. WILTSHIRE. 1999. Trimethylamine induces migration of waterfleas. *Nature* **398**: 382.
- KLÜTTGEN, B., U. DÜLMER, M. ENGELS, AND H. T. RATTE. 1994. ADaM, an artificial freshwater for the culture of zooplankton. *Water Res.* **28**: 743–746.
- LOOSE, C. J., E. VON ELERT, AND P. DAWIDOWICZ. 1993. Chemically-induced diel vertical migration in *Daphnia*: A new bioassay for kairomones exuded by fish. *Arch. Hydrobiol.* **126**: 329–337.
- NEWMAN, J. A., J. BERGELSON, AND A. GRAFEN. 1997. Blocking factors and hypothesis tests in ecology: Is your statistics text wrong? *Ecology* **78**: 1312–1320.
- REEDE, T. 1995. Life history shifts in response to different levels of fish kairomones in *Daphnia*. *J. Plankton Res.* **17**: 1661–1667.
- STIBOR, H. 1992. Predator induced life-history shifts in a freshwater cladoceran. *Oecologia* **92**: 162–165.
- TOLLRIAN, R., AND S. I. DODSON. 1999. Inducible defenses in Cladocera: Constraints, costs, and multipredator environments, p. 177–202. *In* R. Tollrian and C. D. Harvell [eds.], *The ecology and evolution of inducible defenses*. Princeton Univ. Press.
- VON ELERT, E., AND C. J. LOOSE. 1996. Predator-induced diel vertical migration in *Daphnia*: Enrichment and preliminary chemical characterization of a kairomone exuded by fish. *J. Chem. Ecol.* **22**: 885–895.

Received: 13 October 1999

Accepted: 31 January 2000

Amended: 8 February 2000

modeling of the natural <sup>210</sup>Pb cycle. Lead-210 found in sediments has two components: the supported <sup>210</sup>Pb, which originates from the <sup>222</sup>Rn decay that occurs in the sediment, and the unsupported <sup>210</sup>Pb, which originates from the <sup>222</sup>Rn decay that occurs in the atmosphere and the water column. The activity profile of the unsupported component is the input data for <sup>210</sup>Pb dating models, which are used to estimate the chronology of the sediment (Appleby and Oldfield 1978). Although modeling of the <sup>210</sup>Pb cycle would be desirable for dating purposes, dating models generally use rough assumptions on the sedimentation processes.

The aim of this work is to revise the basic assumptions of the constant rate of supply (CRS) model (Appleby and Oldfield 1978) and to explore the validity of its mass flux (sedimentation rate) formula.

**Review of the CRS model**—One of the most widely used <sup>210</sup>Pb sediment dating models is the CRS model. This model is based on the assumption that there is a constant rate of

Table 1. Nomenclature of formulae included in the text.

Nomenclature	Interpretation
$\lambda$	$^{210}\text{Pb}$ decay constant ( $\text{yr}^{-1}$ )
$\alpha$	Constant rate of supply of unsupported $^{210}\text{Pb}$ to the sediment ( $\text{Bq m}^{-2} \text{ yr}^{-1}$ )
$\alpha'$	Inventory of unsupported $^{210}\text{Pb}$ in the first section ( $\text{Bq m}^{-2}$ )
$\alpha(t)$	Variable rate of supply of unsupported $^{210}\text{Pb}$ to the sediment ( $\text{Bq m}^{-2} \text{ yr}^{-1}$ )
$\Delta t$	Time interval (yr)
$A(0)$	Total inventory of unsupported $^{210}\text{Pb}$ ( $\text{Bq m}^{-2}$ )
$A(x)$	Inventory of unsupported $^{210}\text{Pb}$ from depth $x$ to the bottom of the sediment ( $\text{Bq m}^{-2}$ )
$A_c(t)$	Inventory of unsupported $^{210}\text{Pb}$ from the surface during time $t$ ( $\text{Bq m}^{-2}$ )
$C(x)$	Activity of unsupported $^{210}\text{Pb}$ ( $\text{Bq kg}^{-1}$ ) at depth $x$
$C_0$	Activity of unsupported $^{210}\text{Pb}$ ( $\text{Bq kg}^{-1}$ ) in the first section
$C'_0$	Initial activity of unsupported $^{210}\text{Pb}$ ( $\text{Bq kg}^{-1}$ ) in the first section
$n$	Number of time intervals
$q$	Supply of unsupported $^{210}\text{Pb}$ to the sediment ( $\text{Bq m}^{-2} \text{ yr}^{-1}$ ) in the PF model
$r$	Mass flux ( $\text{kg m}^{-2} \text{ yr}^{-1}$ )
$r'$	Mass flux during the formation of the first section ( $\text{kg m}^{-2} \text{ yr}^{-1}$ )
$t$	Age (yr)
$T$	Number of years required to form a section (formation period)
$x$	Depth (m)

supply of unsupported  $^{210}\text{Pb}$  to the sediment. The inventory ( $\text{Bq m}^{-2}$ ) of unsupported  $^{210}\text{Pb}$  from depth  $x$  (age  $t$ ) to the bottom of the sediment column is

$$A(x) = \int_t^\infty \alpha \cdot e^{-\lambda t} dt = A(0) \cdot e^{-\lambda x} \quad (1)$$

where  $A(0)$  is the total inventory of unsupported  $^{210}\text{Pb}$ ,  $\alpha$  ( $\text{Bq m}^{-2} \text{ yr}^{-1}$ ) is the constant rate of supply of unsupported  $^{210}\text{Pb}$  to the sediment, and  $\lambda$  is the  $^{210}\text{Pb}$  decay constant ( $0.03114 \text{ yr}^{-1}$ ). A full nomenclature list can be found in Table 1. The equation

$$A(0) = \frac{\alpha}{\lambda} \quad (2)$$

relates the total inventory  $A(0)$  and the flux  $\alpha$ . From Eq. 1 it is found that

$$t = \frac{1}{\lambda} \cdot \ln\left(\frac{A(0)}{A(x)}\right). \quad (3)$$

In addition, Appleby and Oldfield (1978) provide a formula to determine the mass flux. Let us designate  $r$  as the mass flux ( $\text{kg m}^{-2} \text{ yr}^{-1}$ ) in a section at depth  $x$ ,  $A(x)$  as the inventory ( $\text{Bq m}^{-2}$ ) of unsupported  $^{210}\text{Pb}$  below depth  $x$ , and  $C(x)$  as the activity ( $\text{Bq kg}^{-1}$ ) of unsupported  $^{210}\text{Pb}$  for that section. Thus, the unsupported  $^{210}\text{Pb}$  flux to the first section is

$$rC_0 = \alpha. \quad (4)$$

Because of radioactive decay, the relationship between  $C_0$  and  $C(x)$  is

$$C_0 = C(x)e^{\lambda x}. \quad (5)$$

From Eqs. 1 and 2 it can be shown that

$$\alpha = A(0)\lambda = A(x)e^{\lambda x}\lambda. \quad (6)$$

And, finally, by substituting  $C_0$  and  $\alpha$  (Eqs. 5 and 6) in Eq. 4, the mass flux formula is

$$r = \frac{\lambda \cdot A(x)}{C(x)}. \quad (7)$$

Sedimentation rates,  $v$  ( $\text{m yr}^{-1}$ ), are found by dividing the mass flux in a section by its dry density,  $\rho$  ( $\text{kg m}^{-3}$ ).

This paper discusses the chronology (Eq. 3) and the mass flux (Eq. 7) proposed in the CRS model.

*Proposed model: PF (periodic flux)*—First of all, it was noticed that the use of integrals in Eq. 1 intrinsically implies the assumption of a continuously constant supply of unsupported  $^{210}\text{Pb}$  in the CRS model. Our first objective was to check that the chronology (Eq. 3) is still valid when considering a more general hypothesis. There are several studies dealing with the  $^{210}\text{Pb}$  supply mechanisms to sediments (Turkian et al. 1977; Tsunogai et al. 1988; Heussner et al. 1990; Thunell and Moore 1994) that show that the unsupported  $^{210}\text{Pb}$  flux to the sediment is time dependent, although the annual variations are possibly small. For this reason we considered the CRS hypothesis, which assumes  $\alpha(t)$  is constant, to be too rigid, and we proposed a more general hypothesis: the supply of unsupported  $^{210}\text{Pb}$  during a period of time  $\Delta t$  (order of magnitude of years) is a constant  $q$  ( $\text{Bq m}^{-2} \text{ yr}^{-1}$ ). We named this hypothesis periodic flux (PF).

Considering the PF hypothesis, the accumulated activity per square meter  $A_c(t)$  from the surface sediment to a depth  $x$  during a time  $t = n\Delta t$  ( $n = 0, 1, 2, \dots$ ) was given by

$$A_c(t = n \cdot \Delta t) = \Delta t \cdot q \cdot (1 + e^{-\lambda \Delta t} + e^{-\lambda 2\Delta t} + \dots + e^{-\lambda (n-1)\Delta t}) \quad (8)$$

where  $q$  ( $\text{Bq m}^{-2} \text{ yr}^{-1}$ ) was the unsupported  $^{210}\text{Pb}$  supply. Solving the series we obtained

$$A_c(t = n \cdot \Delta t) = \Delta t \cdot q \cdot \sum_{k=0}^{n-1} (e^{-\lambda \Delta t})^k = \Delta t \cdot q \cdot \frac{1 - e^{-\lambda \Delta t \cdot n}}{1 - e^{-\lambda \Delta t}}. \quad (9)$$

The sum to an infinite time provided the total inventory  $A(0)$  of unsupported  $^{210}\text{Pb}$  in the sediment column

$$A(0) = \Delta t \cdot q \cdot \sum_{k=0}^{\infty} (e^{-\lambda \Delta t})^k = \Delta t \cdot q \cdot \frac{1}{1 - e^{-\lambda \Delta t}}. \quad (10)$$

In order to obtain  $A(x)$ , the inventory of unsupported  $^{210}\text{Pb}$  from the bottom to depth  $x$ ,  $A_c(x)$  was subtracted from  $A(0)$

$$A(x) = \Delta t \cdot q \cdot \frac{1}{1 - e^{-\lambda \Delta t}} \cdot e^{-\lambda \cdot n \Delta t} = A(0) \cdot e^{-\lambda \cdot n \Delta t} \quad (11)$$

and, thus, we obtained the following PF chronology formula

$$t(\equiv n \cdot \Delta t) = \frac{1}{\lambda} \cdot \ln\left(\frac{A(0)}{A(x)}\right) \quad (12)$$

which is identical to the CRS chronology formula.

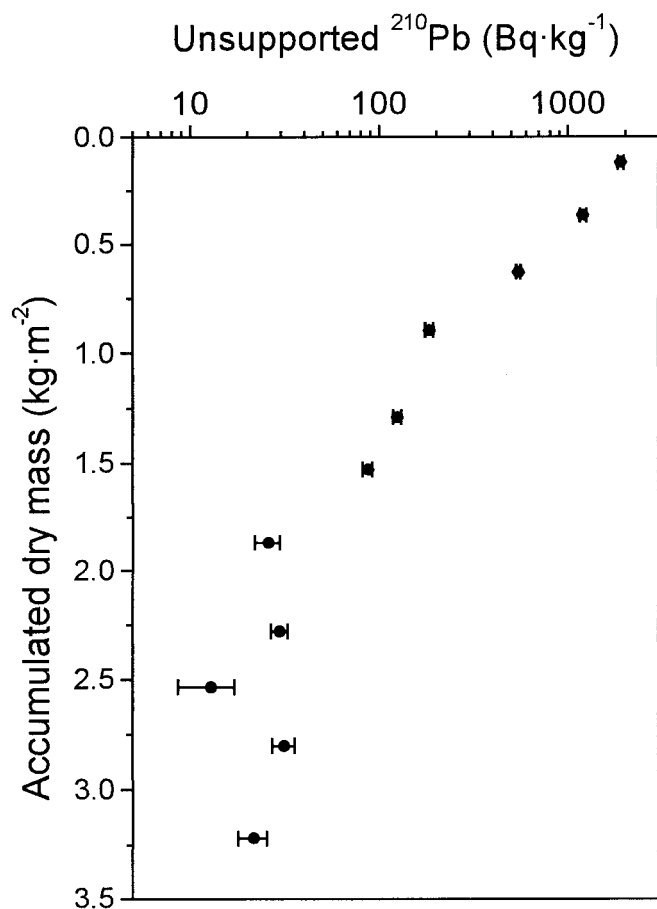


Fig. 1. Activity profile of unsupported  $^{210}\text{Pb}$ , core Redó-1, Central Pyrenees (Spain).

*Discussion of the chronology formulae*—We showed that the chronology formula proposed in the CRS model is correct even if the supply of unsupported  $^{210}\text{Pb}$  is constant every  $\Delta t$  years instead of being continuously constant. We concluded that the success of the CRS chronology formula is

due to the fact that the chronology is not dependent on  $\Delta t$ , as can be seen from Eq. 12.

It is worth noting that the CRS model is a particular case of the PF model: when the interval  $\Delta t$  becomes infinitesimal, the more general discontinuous formulae (PF model) tend to the particular continuous formulae (CRS model). Eq. 2 of the CRS model is the particular case, when  $\Delta t \rightarrow 0$ , of Eq. 10 of the PF model. If we consider the PF hypothesis to be valid, the flux can be obtained from the following formula:

$$q = \frac{A(0)}{\Delta t} \cdot (1 - e^{-\lambda \Delta t}). \quad (13)$$

To determine the flux  $q$  we need to know the interval  $\Delta t$ . If in a particular location experimental data on unsupported  $^{210}\text{Pb}$  flux to the sediment exist, it should be possible to find the time period  $\Delta t$  for which the supply can be considered constant and then determine the flux  $q$ . If experimental data are not available, we propose to choose the interval  $\Delta t$  as 1 yr according to climate cycles. For example, Biscaye et al. (1988) showed that the unsupported  $^{210}\text{Pb}$  fluxes present a periodical behavior with seasonal variations and annual supplies mainly constant. The use of Eq. 13 instead of Eq. 2 to calculate the unsupported  $^{210}\text{Pb}$  flux to the sediment provides different flux estimates. For example, considering  $\Delta t = 1$  yr, the fluxes determined by the CRS and PF models differ only 1.6% due to the difference between  $\lambda$  and  $[1 - \exp(-\lambda \Delta t)]/\Delta t$ . For longer periods, this difference would be larger: for example, for  $\Delta t = 5, 10$ , or  $15$  yr, the differences would be as large as 8, 16, and 25%, respectively. This difference does not affect the dating of sediments because the flux does not appear in the chronology Eqs. 3 or 12.

*Deduction of the mass flux formula*—We pointed out earlier that the use of integrals in Eq. 1 implied the intrinsic assumption of a continuously constant supply of unsupported  $^{210}\text{Pb}$  in the CRS model. For this reason Eq. 4 is assumed to be valid for infinitesimal periods in the CRS model, which imposes a constraint on the  $rC_0$  product. During these infinitesimal periods, the sediment column grows infinitesimal

Table 2. CRS model dating (Eq. 3) and mass fluxes calculated from the CRS model (Eq. 7), the CRS chronology (Eq. 18), and the PF model (Eq. 17) of core Redó-1, Central Pyrenees. Uncertainties correspond to  $\pm 1 \sigma$ .

Depth (cm)	Dry mass (g m <sup>-2</sup> )	Chronology (Eq. 3) (yr)	Formation period (yr)	Mass flux (Eq. 7) (g m <sup>-2</sup> yr <sup>-1</sup> )	Mass flux (Eq. 18) (g m <sup>-2</sup> yr <sup>-1</sup> )	Mass flux (Eq. 17) (g m <sup>-2</sup> yr <sup>-1</sup> )
0.0	121	1994*	10.4 ± 0.9	13.6 ± 0.5	11.6 ± 1.0	11.6 ± 0.5
0.3	246	1984 ± 1	21.8 ± 1.3	15.6 ± 0.7	11.3 ± 0.7	11.3 ± 0.5
0.6	261	1962 ± 1	20 ± 14	17.3 ± 0.6	12.8 ± 0.9	12.8 ± 0.5
0.9	268	1941 ± 1	11.8 ± 1.7	27.1 ± 1.5	23 ± 3	22.7 ± 1.4
1.2	396	1930 ± 1	19 ± 2	27.8 ± 1.7	21 ± 2	21.1 ± 1.4
1.5	237	1911 ± 2	13 ± 3	22.3 ± 1.7	18 ± 4	18.4 ± 1.6
1.8	339	1898 ± 2	8 ± 3	50 ± 8	45 ± 20	45 ± 8
2.1	412	1890 ± 3	15 ± 4	34 ± 4	27 ± 8	27 ± 4
2.4	255	1875 ± 3	5 ± 5	50 ± 17	46 ± 40	46 ± 20
2.7	267	1870 ± 4	21 ± 7	17 ± 3	13 ± 4	13 ± 3
3.0	417	1849 ± 6	†	13 ± 3	†	†

\* Core surface: date corresponds to sampling date.

† Formation period of the last section is not available because the CRS model does not provide the age of the bottom of the unsupported  $^{210}\text{Pb}$  profile.

Table 3. Mass fluxes calculated from the CRS model (Eq. 7), the CRS chronology (Eq. 18), and the PF model (Eq. 17) of core A6, Bransfield Strait, Antarctica. Uncertainties correspond to  $\pm 1 \sigma$ .

Depth (cm)	Mass flux (Eq. 7) (kg m <sup>-2</sup> yr <sup>-1</sup> )	Mass flux (Eq. 18) (kg m <sup>-2</sup> yr <sup>-1</sup> )	Mass flux (Eq. 17) (kg m <sup>-2</sup> yr <sup>-1</sup> )
0.0	1.64 ± 0.08	1.6 ± 0.5	1.59 ± 0.08
1.0	1.60 ± 0.08	1.6 ± 1.1	1.57 ± 0.08
1.5	1.22 ± 0.06	1.2 ± 0.7	1.20 ± 0.07
2.0	1.33 ± 0.07	1.3 ± 0.8	1.30 ± 0.07
2.5	1.39 ± 0.07	1.4 ± 0.9	1.36 ± 0.07
3.0	1.29 ± 0.06	1.3 ± 0.8	1.26 ± 0.07
3.5	1.73 ± 0.09	1.7 ± 1.1	1.70 ± 0.09
4.0	1.43 ± 0.07	1.4 ± 0.8	1.40 ± 0.07
4.5	1.45 ± 0.07	1.4 ± 0.8	1.41 ± 0.07
5.0	1.16 ± 0.07	1.1 ± 0.5	1.12 ± 0.07
5.5	1.15 ± 0.07	1.1 ± 0.5	1.11 ± 0.07
6.0	1.08 ± 0.06	1.0 ± 0.4	1.04 ± 0.06
6.5	0.94 ± 0.05	0.9 ± 0.3	0.90 ± 0.05
7.0	0.98 ± 0.06	0.9 ± 0.4	0.95 ± 0.06
7.5	0.85 ± 0.05	0.8 ± 0.3	0.82 ± 0.05
8.0	0.99 ± 0.06	1.0 ± 0.5	0.96 ± 0.06
8.5	0.87 ± 0.06	0.8 ± 0.4	0.84 ± 0.06
9.0	1.22 ± 0.08	1.2 ± 0.8	1.18 ± 0.08
9.5	0.89 ± 0.06	0.9 ± 0.3	0.85 ± 0.06
10.0	0.79 ± 0.05	0.71 ± 0.14	0.71 ± 0.05
11.0	0.64 ± 0.05	0.56 ± 0.09	0.56 ± 0.05
12.0	0.69 ± 0.05	0.60 ± 0.10	0.60 ± 0.04
13.0	0.71 ± 0.06	0.63 ± 0.14	0.63 ± 0.05
14.0	0.67 ± 0.06	0.57 ± 0.09	0.57 ± 0.05
15.0	0.72 ± 0.07	0.64 ± 0.17	0.64 ± 0.06
16.0	0.52 ± 0.04	0.42 ± 0.07	0.42 ± 0.04
17.0	0.51 ± 0.05	0.41 ± 0.10	0.41 ± 0.05
18.0	0.43 ± 0.06	0.34 ± 0.08	0.34 ± 0.05
19.0	0.38 ± 0.07	0.30 ± 0.11	0.30 ± 0.06
20.0	0.53 ± 0.14	0.5 ± 0.3	0.46 ± 0.13
21.0	0.45 ± 0.11	0.36 ± 0.19	0.36 ± 0.10
22.0	0.34 ± 0.12	0.26 ± 0.17	0.26 ± 0.10
23.0	0.22 ± 0.11	0.13 ± 0.06	0.13 ± 0.07
24.0	0.14 ± 0.09	*	*

\* Formation period of the last section is not available because the CRS model does not provide the age of the bottom of the unsupported <sup>210</sup>Pb profile.

lengths. Although whole sections require several years to be formed, during which  $r$  and  $C_0$  are assumed to vary, experiments only permit the determination of  $C(x)$ , which corresponds to whole sections. Consequently, we suggest a different interpretation of Eq. 4 in order to find the mass flux formula.

For the most superficial section formed during  $T$  yr, we have that

$$r' C'_0(x) = \alpha', \quad (14)$$

where  $r'$  (kg m<sup>-2</sup>) stands for the mass supplied during the formation period of the section ( $T$  yr),  $C'_0(x)$  (Bq kg<sup>-1</sup>) is the initial activity of the section, and  $\alpha'$  (Bq m<sup>-2</sup>) is the unsupported <sup>210</sup>Pb inventory for that section. The formation period  $T$  is calculated as the age difference between the upper and lower limit of each section. When we considered a constant rate of supply of unsupported <sup>210</sup>Pb to the sediment,  $\alpha$  (Bq m<sup>-2</sup> yr<sup>-1</sup>), we found that

Table 4. Mass fluxes calculated from the CRS model (Eq. 7), the CRS chronology (Eq. 18), and the PF model (Eq. 17) of core EB-2, Foix canyon, Northwestern Mediterranean Sea. Uncertainties correspond to  $\pm 1 \sigma$ .

Depth (cm)	Mass flux (Eq. 7) (kg m <sup>-2</sup> yr <sup>-1</sup> )	Mass flux (Eq. 18) (kg m <sup>-2</sup> yr <sup>-1</sup> )	Mass flux (Eq. 17) (kg m <sup>-2</sup> yr <sup>-1</sup> )
0.0	2.83 ± 0.18	3 ± 3	2.80 ± 0.18
0.5	3.0 ± 0.2	3 ± 2	3.0 ± 0.2
1.0	2.67 ± 0.16	2.6 ± 1.5	2.61 ± 0.16
1.5	2.88 ± 0.16	2.8 ± 1.6	2.81 ± 0.16
2.0	3.18 ± 0.16	3.1 ± 1.7	3.10 ± 0.16
2.5	2.86 ± 0.19	2.8 ± 1.7	2.80 ± 0.19
3.0	3.2 ± 0.2	3.7 ± 1.8	3.2 ± 0.2
3.5	3.5 ± 0.2	3 ± 2	3.4 ± 0.2
4.0	3.5 ± 0.3	3 ± 2	3.4 ± 0.3
4.5	3.6 ± 0.2	3 ± 2	3.5 ± 0.2
5.0	3.3 ± 0.2	3.2 ± 1.9	3.2 ± 0.2
5.5	3.1 ± 0.2	3.0 ± 1.9	3.0 ± 0.2
6.0	2.62 ± 0.16	2.6 ± 1.5	2.55 ± 0.17
6.5	2.36 ± 0.16	2.3 ± 1.3	2.29 ± 0.16
7.0	2.38 ± 0.13	2.3 ± 1.2	2.30 ± 0.13
7.5	2.36 ± 0.17	2.3 ± 1.3	2.29 ± 0.17
8.0	2.38 ± 0.15	2.3 ± 1.4	2.30 ± 0.15
8.5	2.33 ± 0.14	2.3 ± 1.3	2.25 ± 0.14
9.0	2.17 ± 0.13	2.1 ± 1.3	2.10 ± 0.14
9.5	2.34 ± 0.14	2.3 ± 1.6	2.26 ± 0.14
10.0	2.38 ± 0.19	2.2 ± 0.8	2.23 ± 0.19
11.0	2.10 ± 0.17	2.0 ± 0.8	1.97 ± 0.17
12.0	1.49 ± 0.12	1.3 ± 0.3	1.34 ± 0.11
13.0	1.80 ± 0.16	1.7 ± 0.6	1.65 ± 0.15
14.0	1.76 ± 0.17	1.6 ± 0.5	1.57 ± 0.16
15.0	1.7 ± 0.2	1.6 ± 0.6	1.57 ± 0.19
16.0	1.7 ± 0.2	1.5 ± 0.6	1.5 ± 0.2
17.0	1.21 ± 0.15	1.1 ± 0.3	1.06 ± 0.14
18.0	1.12 ± 0.15	1.0 ± 0.3	0.96 ± 0.14
19.0	1.1 ± 0.2	1.0 ± 0.4	0.97 ± 0.18
20.0	1.5 ± 0.3	1.3 ± 0.8	1.3 ± 0.3
21.0	1.1 ± 0.2	0.9 ± 0.5	0.9 ± 0.2
22.0	0.8 ± 0.2	0.7 ± 0.3	0.66 ± 0.18
23.0	0.46 ± 0.12	0.29 ± 0.12	0.29 ± 0.09
24.0	0.5 ± 0.3	0.28 ± 0.18	0.28 ± 0.17
25.0	0.3 ± 0.3	*	*

\* Formation period of the last section is not available because the CRS model does not provide the age of the bottom of the unsupported <sup>210</sup>Pb profile.

$$\alpha' = \int_0^T \alpha \cdot e^{-\lambda t} dt = \frac{\alpha}{\lambda} (1 - e^{-\lambda T}) \quad (15)$$

whereas the relation between mass supply  $r'$  (kg m<sup>-2</sup>) and mass flux corresponding to the whole section,  $r$  (kg m<sup>-2</sup> yr<sup>-1</sup>), was

$$r' = rT. \quad (16)$$

From Eqs. 14, 15, 5, and 6 we deduced that

$$r = \frac{r'}{T} = \frac{A(x)}{T \cdot C(x)} (1 - e^{-\lambda T}). \quad (17)$$

This formula is different from that in Eq. 7 proposed with the CRS model. If the product  $\lambda T$  was small, we could perform Taylor's expansion of the exponential function in Eq.

17, and, considering only the first two terms of the expansion, we would regain Eq. 7. However, the assumption of  $\lambda T$  as small is usually not valid because  $T$  may represent several years and  $\lambda = 0.03114 \text{ yr}^{-1}$ . Thus, Eq. 17 is different from the commonly used Eq. 7.

*Discussion of the mass flux formula*—In order to validate Eq. 17, we applied the new model, among others, to the sediment core Redó-1. This core was sampled in August 1994 from the deepest part of Redó lake, an alpine lake located in the Central Pyrenees (Catalan 1987). Sampling, treatment, laboratory methods, and dating are described in detail in Masqué (1995), Ani-Ragolta (1996), and Sanchez-Cabeza et al. (1998). The activity profile of unsupported  $^{210}\text{Pb}$  is shown in Fig. 1. The results of the CRS model dating using Eqs. 3 and 7 are presented in Table 2.

Regarding mass fluxes, it should be noted that there is an indirect way to calculate the mass flux, dividing the mass of each section by its formation period obtained from the core chronology (Sanchez-Cabeza et al. 1993)

$$r = \frac{m}{T}. \quad (18)$$

This should coincide with that obtained using the mass sedimentation formulae in any sediment profile dating (Eq. 17). The mass fluxes calculated in this way, and shown in Table 2, differed from those obtained from the CRS model but were identical to those obtained from the PF model. Differences were as large as 38% in section 2. As expected, the largest differences were observed for those sections showing longest formation periods. It is worth to point out that although the CRS chronology does not permit us to assign an age to the bottom of the  $^{210}\text{Pb}$  unsupported profile, the CRS model, through Eq. 7, assigns a mass flux to the deepest section.

Uncertainties were computed throughout the work by the well-known quadratic uncertainty propagation method; the number of significant figures reported was 2 when the first significant figure was 1, and 1 in the other cases. The number of significant figures of each result was adjusted to the last decimal place of the uncertainty.

The mass fluxes obtained through the use of Eq. 18 were, in general, accompanied by large uncertainties (Table 2) because chronology uncertainties are accumulated in the calculation. We present the mass fluxes calculated by using Eq. 17 in Table 2. These values are identical to those calculated from the CRS chronology, which confirms the validity of Eq. 17 for determining mass flux calculations. Furthermore, the associated errors obtained through this expression were significantly smaller than those obtained from the chronology. Investigators using Eq. 18 are not suffering thus any inaccuracy in their conclusions but are overestimating the uncertainty of the results.

The validity of these conclusions was tested in other cores collected from various marine environments. These were (1) core A-3 (Table 3), collected from the Bransfield strait (Antarctica) (Masqué et al. in prep.), (2) core EB-2 (Table 4), collected from the Foix canyon (Northwestern Mediterranean Sea) (Sanchez-Cabeza et al. 1999), (3) core T-1 (Table 5), collected from the Alboran Sea (Mediterranean Sea)

Table 5. Mass fluxes calculated from the CRS model (Eq. 7), the CRS chronology and the PF model (Eq. 17) of core T-1, Alboran Sea, Mediterranean Sea. Uncertainties correspond to  $\pm \sigma$ .

Depth (cm)	Mass flux (Eq. 7) (kg m <sup>-2</sup> yr <sup>-1</sup> )	Mass flux (Eq. 18) (kg m <sup>-2</sup> yr <sup>-1</sup> )	Mass flux (Eq. 17) (kg m <sup>-2</sup> yr <sup>-1</sup> )
0.0	1.13 ± 0.07	1 ± 1	1.12 ± 0.07
0.5	0.83 ± 0.05	0.8 ± 0.5	0.81 ± 0.05
1.0	1.17 ± 0.08	1.1 ± 0.9	1.15 ± 0.08
1.5	1.07 ± 0.06	1.0 ± 0.5	1.03 ± 0.06
2.0	1.08 ± 0.08	1.0 ± 0.5	1.04 ± 0.08
2.5	1.16 ± 0.07	1.1 ± 0.6	1.12 ± 0.07
3.0	1.14 ± 0.08	1.1 ± 0.5	1.09 ± 0.08
3.5	1.30 ± 0.08	1.3 ± 0.6	1.25 ± 0.08
4.0	1.52 ± 0.13	1.5 ± 1.0	1.48 ± 0.13
4.5	1.41 ± 0.09	1.4 ± 0.8	1.36 ± 0.10
5.0	1.89 ± 0.17	1.8 ± 1.5	1.84 ± 0.17
5.5	1.54 ± 0.09	1.5 ± 1.0	1.49 ± 0.09
6.0	1.75 ± 0.14	1.7 ± 1.2	1.70 ± 0.14
6.5	1.50 ± 0.13	1.5 ± 1.0	1.45 ± 0.13
7.0	1.41 ± 0.13	1.3 ± 0.7	1.35 ± 0.13
7.5	1.85 ± 0.17	1.8 ± 1.7	1.80 ± 0.17
8.0	1.36 ± 0.10	1.3 ± 0.7	1.31 ± 0.10
8.5	1.51 ± 0.13	1.5 ± 1.1	1.46 ± 0.13
9.0	1.22 ± 0.09	1.2 ± 0.7	1.16 ± 0.09
9.5	1.47 ± 0.16	1.4 ± 1.0	1.42 ± 0.16
10.0	1.58 ± 0.14	1.5 ± 0.6	1.47 ± 0.14
11.0	1.17 ± 0.12	1.1 ± 0.4	1.06 ± 0.12
12.0	1.29 ± 0.16	1.2 ± 0.4	1.17 ± 0.15
13.0	1.31 ± 0.19	1.2 ± 0.5	1.19 ± 0.18
14.0	1.05 ± 0.14	0.9 ± 0.4	0.94 ± 0.13
15.0	0.94 ± 0.11	0.8 ± 0.3	0.82 ± 0.11
16.0	0.76 ± 0.10	0.6 ± 0.2	0.64 ± 0.09
17.0	0.77 ± 0.16	0.7 ± 0.3	0.66 ± 0.15
18.0	0.54 ± 0.11	0.4 ± 0.2	0.41 ± 0.10
19.0	0.31 ± 0.08	0.18 ± 0.06	0.18 ± 0.05
20.0	0.21 ± 0.10	*	*

\* Formation period of the last section is not available because the CRS model does not provide the age of the bottom of the unsupported  $^{210}\text{Pb}$  profile.

(Masqué et al. in prep.), and (4) core TG8 (Table 6), collected from the Besòs pro-delta (Northwestern Mediterranean Sea) (Palanques et al. 1998).

As was shown for core Redó-1, Eqs. 17 and 18 provided in all cases identical mass fluxes but different from those obtained from the CRS model, although the difference was, in general, small because the formation periods were short. Significant differences were observed in core TG-8 (Table 6) because of the lower sedimentation rates, and therefore longer formation times, observed. On the other hand, because sedimentation rates in cores A-3, EB-2, and T-1 were relatively large, the formation period of the sections was small and, therefore, the uncertainty of the mass fluxes obtained from Eq. 18 was excessively large, especially in the top of the cores. In these cases it was evident that the use of Eq. 17 yielded much lower uncertainties, similar to those obtained from the CRS model (Eq. 7).

*Conclusion*—We discussed the chronology and mass flux formulae proposed by the CRS model. Taking into account

Table 6. Mass fluxes calculated from the CRS model (Eq. 7), the CRS chronology (Eq. 18), and the PF model (Eq. 17) of core TG-8, Besòs pro-delta, Northwestern Mediterranean Sea. Uncertainties correspond to  $\pm 1 \sigma$ .

Depth (cm)	Mass flux (Eq. 7) (kg m <sup>-2</sup> yr <sup>-1</sup> )	Mass flux (Eq. 18) (kg m <sup>-2</sup> yr <sup>-1</sup> )	Mass flux (Eq. 17) (kg m <sup>-2</sup> yr <sup>-1</sup> )
0.0	1.94 ± 0.10	1.9 ± 0.6	1.86 ± 0.10
1.0	2.38 ± 0.15	2.3 ± 1.1	2.28 ± 0.15
2.0	2.03 ± 0.13	1.9 ± 0.5	1.88 ± 0.12
3.0	1.93 ± 0.13	1.8 ± 0.6	1.79 ± 0.12
4.0	1.74 ± 0.11	1.6 ± 0.4	1.57 ± 0.11
5.0	1.66 ± 0.12	1.5 ± 0.4	1.51 ± 0.12
6.0	1.57 ± 0.12	1.4 ± 0.3	1.39 ± 0.12
7.0	1.87 ± 0.19	1.7 ± 0.8	1.75 ± 0.19
8.0	1.24 ± 0.11	1.1 ± 0.2	1.05 ± 0.10
9.0	0.91 ± 0.09	0.76 ± 0.18	0.76 ± 0.08
10.0	0.57 ± 0.06	0.38 ± 0.06	0.38 ± 0.05
11.0	0.46 ± 0.08	0.26 ± 0.07	0.26 ± 0.06
12.0	0.40 ± 0.18	*	*

\* Formation period of the last section is not available because the CRS model does not provide the age of the bottom of the unsupported <sup>210</sup>Pb profile.

a more general hypothesis, which we called periodic flux (PF), we obtained the same chronology formula, which is a further confirmation of the CRS hypothesis. We also found that, considering  $\Delta t = 1$  yr, the unsupported <sup>210</sup>Pb flux values proposed by the CRS model are 1.5% higher than those proposed by the PF model. This difference would be larger when considering longer periods.

The dating of core Redó-1 showed significant discrepancies of the mass flux values proposed by the CRS model (Eq. 7) and the CRS chronology (Eq. 18). We deduced a mass flux formula from the PF model (Eq. 17), which provided mass flux values consistent with the CRS chronology but different from those obtained from the CRS model. Also, Eq. 17 generated smaller uncertainties associated with mass flux than Eq. 18 and, therefore, with sedimentation rates. These conclusions were confirmed in other cores from a diverse origin. It was concluded that larger differences between the CRS model (Eq. 7) and the PF model (Eq. 17) mass fluxes were observed in sections with longer formation periods. Also, when comparing mass fluxes obtained from the CRS chronology (Eq. 18) and the PF model (Eq. 17), sections with lower formation periods showed lower uncer-

<sup>1</sup> Corresponding author (JoanAlbert.Sanchez@uab.es).

#### Acknowledgments

The authors wish to acknowledge financial support received to carry out this work from the Comisión Interministerial de Ciencia y Tecnología (CICYT, Spain, AMB93-0814 and AMB92-0251), European Commission (MTP II-MATER, MAS3-CT96-0051), and ENRESA (Contrato 70.2.4.11.01). Some sediment cores analyzed in this work were collected in the frame of projects financed by the European Commission (Euromarge-NB, MAS2-CT930053) and CICYT (ANT-40/94 and ANT96-1346-E). Special thanks are due to W. R. Schell, who introduced us to this interesting field.

tainties using the PF model. Therefore, the PF model should be preferred to calculate mass fluxes (Eq. 17). Investigators using Eq. 18 are not suffering any inaccuracy in their conclusions, but are overestimating the uncertainty of the results.

J. A. Sanchez-Cabeza<sup>1</sup>  
I. Ani-Ragolta  
P. Masqué

Departament de Física  
Universitat Autònoma de Barcelona  
ES-08193 Bellaterra, Spain

#### References

- ANI-RAGOLTA, I. 1996. <sup>210</sup>Pb en sediments: Estudi i aplicació d'alguns models de datació. Master's dissertation, Autonomus Univ. Barcelona.
- APPLEBY, P. G., AND F. OLDFIELD. 1978. The calculation of <sup>210</sup>Pb dates assuming a constant rate of supply of unsupported <sup>210</sup>Pb to the sediment. *Catena* **5**: 1–8.
- BISCAYE, P. E., R. F. ANDERSON, AND B. L. DECK. 1988. Fluxes of particles and constituents to the eastern United States continental slope and rise: SEEP-I. *Cont. Shelf Res.* **8**: 855–904.
- CATALAN, J. 1987. Limnologia de l'estany Redó (Pirineu Central). Ph.D. dissertation, Univ. Barcelona.
- HEUSSNER, S., R. D. CHERRY, AND M. HEYRAUD. 1990. Po-210, Pb-210 in sediment trap particles on a Mediterranean continental margin. *Cont. Shelf Res.* **10**: 989–1004.
- MASQUÉ, P. 1995. Introducció a la datació de sediments marins mitjançant la tècnica del <sup>210</sup>Pb. Master's dissertation, Autonomus Univ. Barcelona.
- PALANQUES, A., J. A. SANCHEZ-CABEZA, P. MASQUÉ, AND L. LEÓN. 1998. Historical record of heavy metals in a highly contaminated Mediterranean deposit: The Besòs prodelta. *Mar. Chem.* **61**: 209–217.
- SANCHEZ-CABEZA, J. A., AND OTHERS. 1993. A record of anthropogenic environmental impact in the continental shelf north of Barcelona city, p. 175–184. *In* Isotope techniques in the study of past and current environmental changes in the hydrosphere and the atmosphere, IAEA-SM-329/18, Vienna.
- , P. MASQUÉ, AND I. ANI-RAGOLTA. 1998. <sup>210</sup>Pb and <sup>210</sup>Po analysis in sediments and soils by microwave acid digestion. *J. Radioanal. Nucl. Chem.* **227**: 19–22.
- , AND OTHERS. 1999. Sediment accumulation rates in the southern Barcelona continental margin (NW Mediterranean Sea) derived from <sup>210</sup>Pb and <sup>137</sup>Cs chronology, *Prog. Oceanogr.* **44**: 313–332.
- THUNELL, R. C., AND W. S. MOORE. 1994. Elemental and isotopic fluxes in the Southern California Bight: A time-series sediment trap study in the San Pedro Basin. *J. Geophys. Res.* **99**: 875–889.
- TSUNOGAI, S., T. KURATA, T. SUZUKI, AND K. YOKOTA. 1988. Seasonal variation of atmospheric <sup>210</sup>Pb and Al in the Western North Pacific region. *J. Atmos. Chem.* **7**: 389–407.
- TUREKIAN, K. K., Y. NOZAKI, AND L. K. BENNINGER. 1977. Geochemistry of atmospheric radon and radon products. *Annu. Rev. Earth Planet. Sci.* **5**: 227–255.

Received: 12 November 1998

Amended: 6 January 2000

Accepted: 3 February 2000